



Falkland Islands Fisheries Department

Falkland calamari Stock Assessment, 2nd Season 2015

Andreas Winter

September 2015

Index

Summary	3
Introduction.....	3
Methods.....	3
Stock assessment.....	6
Data.....	6
Group arrivals / depletion criteria.....	8
Depletion analyses.....	11
North.....	11
South.....	12
Escapement biomass.....	15
Mortality / Emigration.....	15
Evaluation of season schedule change.....	16
Fishing outside the Loligo Box.....	16
Bycatch	17
References.....	19
Appendix.....	21
Falkland calamari individual weights.....	21
Prior estimates and CV	22
Depletion model estimates and CV	23
Combined Bayesian models	24

Summary

- 1) The 2015 second season Falkland calamari fishery opened on July 29th, one week later than the year before to equalize the first season schedule which had been extended a week longer. The second season was closed by emergency order for stock conservation on September 8th, after 42 fishing days.
- 2) 10,190 tonnes of Falkland calamari catch were reported in the 2015 X-license fishery; the lowest catch for a 2nd season since 2002. Throughout the season 50.9% of calamari catch and 54.5% of fishing effort were taken north of latitude 52° S; 49.1% of calamari catch and 45.5% of effort were taken south of 52° S.
- 3) Sub-areas north and south of 52° S were depletion-modelled separately. No in-season immigrations / depletion periods were inferred in either the north or the south sub-area.
- 4) The final total estimate for calamari remaining in the Loligo Box at the end of second season 2015 was:
Maximum likelihood of 10,703 tonnes, with a 95% confidence interval of [7,486 to 18,762] tonnes.
The risk of calamari escapement biomass at the end of the season being less than 10,000 tonnes was estimated at 29.0%.

Introduction

The second season of the 2015 Falkland calamari fishery (*Doryteuthis gahi* – Patagonian longfin squid – colloquially *Loligo*) opened on July 29th with all 16 X-licensed vessels participating; none taking the flex option to start later. Season opening was one week later than second season of the year before, complementary to the scheduling change of one week having been added to the end of first season (Winter, 2015), and thus completing the phased 2-year equalization between 1st and 2nd season schedules (Fisheries Committee, 2013). The season was closed by emergency order at 23:59 on September 8th. One vessel, with observer on board, took four exploratory fishing days in-season north of the Loligo Box with authorization from the FIFD. Total reported Falkland calamari catch by X-licensed vessels in the 2015 2nd season was 10,190 tonnes in 665 vessel-days (Table 1); obtaining the lowest catch for a 2nd season since 2002 (Payá, 2010) and the lowest catch rate (tonnes / vessel / day) for a 2nd season since 2004.

As in previous seasons, the Falkland calamari stock assessment was conducted with depletion time-series models (Agnew et al., 1998; Roa-Ureta and Arkhipkin, 2007; Arkhipkin et al., 2008). Because Falkland calamari has an annual life cycle (Patterson, 1988), stock cannot be derived from a standing biomass carried over from prior years (Rosenberg et al., 1990). The depletion model instead calculates an estimate of population abundance over time by evaluating what levels of abundance and catchability must be extant to sustain the observed rate of catch. Depletion modelling is used both in-season and for the post-season summary, with the objective of maintaining an escapement biomass of 10,000 tonnes Falkland calamari at the end of each season as a conservation threshold (Agnew et al., 2002; 2005; Barton, 2002).

Methods

The depletion model formulated for the Falkland calamari stock is based on the equivalence:

$$C_{\text{day}} = q \times E_{\text{day}} \times N_{\text{day}} \times e^{-M/2} \quad (1)$$

where q is the catchability coefficient, M is the natural mortality rate (considered constant at 0.01333 day^{-1} ; Roa-Ureta and Arkhipkin, 2007), and C_{day} , E_{day} , N_{day} are catch (numbers of calamari), fishing effort (numbers of vessels), and abundance (numbers of calamari) per day. In its basic form (DeLury, 1947) the depletion model assumes a closed population in a fixed area for the duration of the assessment. However, the assumption of a closed population is imperfectly met in the Falkland Islands fishery, where stock analyses have often shown that calamari groups arrive in successive waves after the start of the season (Roa-Ureta, 2012; Winter and Arkhipkin, 2015). Arrivals of successive groups are inferred from discontinuities in the catch data. Fishing on a single, closed cohort would be expected to yield gradually decreasing CPUE, but gradually increasing average individual sizes, as the squid grow. When instead these data change suddenly, or in contrast to expectation, the immigration of a new group to the population is indicated.

In the event of a new group arrival, the depletion calculation must be modified to account for this influx. This is implemented using a simultaneous algorithm (Roa-Ureta, 2012) that adds new arrivals on top of the stock previously present, and posits a common catchability coefficient for the entire depletion time-series. If two depletions are included in the same model (i.e., the stock present from the start plus a new group arrival), then:

$$C_{\text{day}} = q \times E_{\text{day}} \times (N1_{\text{day}} + (N2_{\text{day}} \times i2_{|0}^1)) \times e^{-M/2} \quad (2)$$

where $i2$ is a dummy variable taking the values 0 or 1 if 'day' is before or after the start day of the second depletion. For more than two depletions, $N3_{\text{day}}$, $i3$, $N4_{\text{day}}$, $i4$, etc., would be included following the same pattern.

Table 1. Falkland calamari season comparisons since 2004. Days: total number of calendar days open to licensed Falkland calamari fishing including (since 1st season 2013) optional extension days; V-Days: aggregate number of licensed Falkland calamari fishing days reported by all vessels for the season.

Year	Season 1			Season 2		
	Catch (t)	Days	V-Days	Catch (t)	Days	V-Days
2004				17,559	78	1271
2005	24,605	45	576	29,659	78	1210
2006	19,056	50	704	23,238	53	883
2007	17,229	50	680	24,171	63	1063
2008	24,752	51	780	26,996	78	1189
2009	12,764	50	773	17,836	59	923
2010	28,754	50	765	36,993	78	1169
2011	15,271	50	771	18,725	70	1099
2012	34,767	51	770	35,026	78	1095
2013	19,908	53	782	19,614	78	1195
2014	28,119	59	872	19,630	71	1099
2015	19,383*	57*	871*	10,190	42	665

* Does not include C-license catch or effort after the C-license target for that season was switched from *D. gahi* to *Illex*.

The Falkland calamari stock assessment was calculated in a Bayesian framework (Punt and Hilborn, 1997), whereby results of the season depletion model are conditioned by prior information on the stock; in this case the information from the pre-season survey. The season depletion likelihood function was calculated as the difference between actual catch numbers reported and catch numbers predicted from the model (equation 2), statistically corrected by a factor relating to the number of days of the depletion period (Roa-Ureta, 2012):

$$\left((n\text{Days} - 2) / 2 \right) \times \log \left(\sum_{\text{days}} \left(\log(\text{predicted } C_{\text{day}}) - \log(\text{actual } C_{\text{day}}) \right)^2 \right) \quad (3)$$

The survey prior likelihood function was calculated as the normal distribution of the difference between catchability (q) derived from the survey abundance estimate, and catchability derived from the season depletion model:

$$\frac{1}{\sqrt{2\pi \cdot \text{SD}_{q \text{ survey}}^2}} \times \exp \left(- \frac{(q_{\text{model}} - q_{\text{survey}})^2}{2 \cdot \text{SD}_{q \text{ survey}}^2} \right) \quad (4)$$

Catchability, rather than abundance N , was used for calculating the survey prior likelihood because catchability informs the entire season time series; whereas N from the survey only informs the first season depletion period – subsequent immigrations and depletions are independent of the abundance that was present during the survey.

Bayesian optimization of the depletion was calculated by jointly minimizing equations 3 and 4, using the Nelder-Mead algorithm in R programming package ‘optimx’ (Nash and Varadhan, 2011). Relative weights in the joint optimization were assigned to equations 3 and 4 as the converse of their coefficients of variation (CV), i.e., the CV of the prior became the weight of the depletion model and the CV of the depletion model became the weight of the prior. Calculations of the CVs are described in the Appendix.

With C_{day} , E_{day} and M being fixed parameters, the optimization of equation 2 using 3 and 4 produces estimates of q and N_1, N_2, \dots , etc. Numbers of calamari on the final day (or any other day) of a time series are then calculated as the numbers N of the depletion start days discounted for natural mortality during the intervening period, and subtracting cumulative catch also discounted for natural mortality (CNMD). Taking for example a two-depletion period:

$$N_{\text{final day}} = N_1_{\text{start day 1}} \times e^{-M(\text{final day} - \text{start day 1})} + N_2_{\text{start day 2}} \times e^{-M(\text{final day} - \text{start day 2})} - \text{CNMD}_{\text{final day}} \quad (5)$$

where

$$\begin{aligned} \text{CNMD}_{\text{day 1}} &= 0 \\ \text{CNMD}_{\text{day x}} &= \text{CNMD}_{\text{day x-1}} \times e^{-M} + C_{\text{day x-1}} \times e^{-M/2} \end{aligned} \quad (6)$$

$N_{\text{final day}}$ is then multiplied by the average individual weight of calamari on the final day to give biomass. Daily average individual weight is obtained from length / weight conversion of mantle lengths measured in-season by observers, and also derived from in-season commercial data as the proportion of product weight that vessels reported per market size category.

Observer mantle lengths are scientifically precise, but restricted to 1-2 vessels at any one time that may or may not be representative of the entire fleet. Commercially proportioned mantle lengths are relatively less precise, but cover the entire fishing fleet. Therefore, both sources of data are used. Daily average individual weights are calculated by averaging observer size samples and commercial size categories where observer data are available, otherwise only commercial size categories. To smooth fluctuations, $N_{\text{final day}}$ (or N on any other day of interest) is multiplied by the expected value of the average individual weight from its GAM trend (see Appendix), rather than by the empirical value on each day.

Distributions of the likelihood estimates from joint optimization (i.e., measures of their statistical uncertainty) were computed using a Markov Chain Monte Carlo (MCMC) (Gamerman and Lopes, 2006), a method that is commonly employed for fisheries assessments (Magnusson et al., 2013). MCMC is an iterative process which generates random stepwise changes to the proposed outcome of a model (in this case, the N and q of calamari) and at each step, accepts or nullifies the change with a probability equivalent to how well the change fits the model parameters compared to the previous step. The resulting sequence of accepted or nullified changes (i.e., the ‘chain’) approximates the likelihood distribution of the model outcome. The MCMC of the depletion models were run for 100,000 iterations; the first 1000 iterations were discarded as burn-in sections (initial phases over which the algorithm stabilizes); and the chains were thinned by a factor equivalent to the maximum of either 5 or the inverse of the acceptance rate (e.g., if the acceptance rate was 12.5%, then every 8th (0.125^{-1}) iteration was retained) to reduce serial correlation. For each model three chains were run; one chain initiated with the parameter values obtained from the joint optimization of equations 3 and 4, one chain initiated with these parameters $\times 2$, and one chain initiated with these parameters $\times \frac{1}{4}$. Convergence of the three chains was accepted if the variance among chains was less than 10% higher than the variance within chains (Brooks and Gelman, 1998). When convergence was satisfied the three chains were combined as one final set. Equations 5, 6, and the multiplication by average individual weight were applied to the CNMD and each iteration of N values in the final set, and the biomass outcomes from these calculations represent the distribution of the estimate. The peaks of the MCMC histograms were compared to the empirical optimizations of the N values.

Total escapement biomass is defined as the aggregate biomass of calamari on the last day of the season for north and south sub-areas combined. Calamari sub-stocks emigrate from different spawning grounds and remain to an extent segregated (Arkhipkin and Middleton, 2002). However, it is not assumed that north and south biomasses are uncorrelated (Shaw et al., 2004), and therefore north and south likelihood distributions were added semi-randomly in proportion to the strength of their day-to-day correlation (see Winter, 2014, for the semi-randomization algorithm).

Stock assessment

Data

Fishing effort in the 2nd season of 2015 was distributed fairly evenly (Figure 1) with 50.9% of calamari catch and 54.5% of effort in the north sub-area (north of 52° S); 49.1% of catch and 45.5% of effort in the south sub-area. The north sub-area includes the vessel that took exploratory fishing north of the Loligo Box. Typical for a mediocre season, the fleet moved back and forth frequently (Figure 2).

A total of 665 vessel-days were fished during the season, with a median of 16 vessels per day. During one day of particularly sustained bad weather (August 18th; Figure 3), fishing effort dropped to less than a third of average. Vessels reported daily catch totals to the FIFD

and electronic logbook data that included trawl times, positions, and product weight by market size categories. Three FIFD observers were deployed on three vessels in the fishery for a total of 52 observer-days (Boag, 2015; Jones, 2015, Jürgens, 2015). Throughout the 42 days of the season, 12 days had no observer covering, 28 days had 1 observer covering, and 12 days had two observers covering. Observers sampled an average of 401.1 calamari daily, and reported their maturity stages, sex, and lengths to 0.5 cm. The length-weight relationship for converting both observer and commercially proportioned length data was taken from the pre-season survey (Jones et al, 2015):

$$\text{weight (kg)} = 0.114 \times \text{length (cm)}^{2.339} / 1000 \quad (7)$$

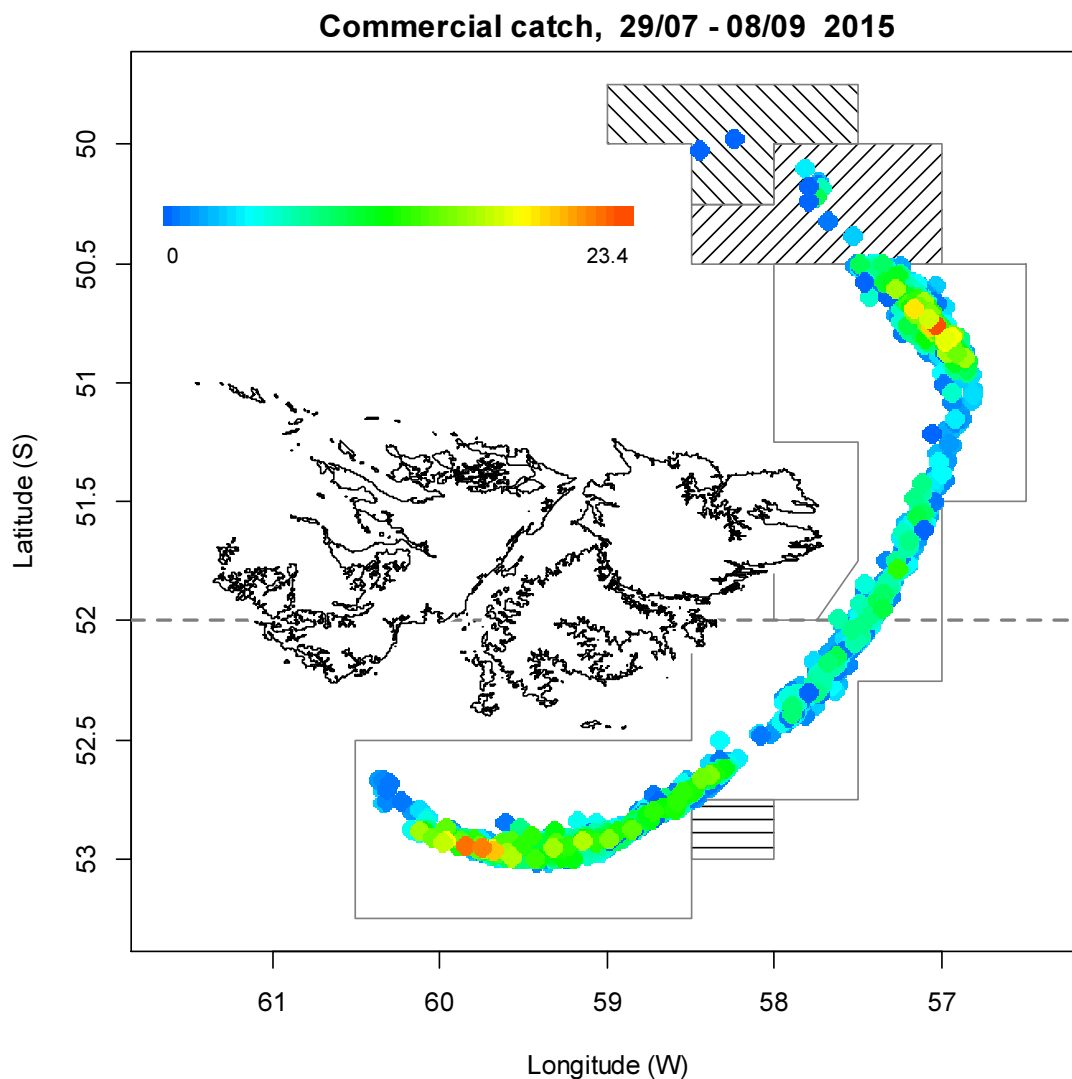


Figure 1. Spatial distribution of Falkland calamari 2nd-season commercial catches, colour-scaled to catch weight (maximum = 23.4 tonnes). 2292 trawl catches were taken during the season. The ‘Loligo Box’ fishing zone is outlined in grey. The adjacent grid shaded horizontally was open to commercial calamari fishing starting Sept. 1st. Grids shaded right-diagonally were open for exploratory calamari fishing to one vessel with observer from Sept. 1st to Sept. 3rd. Grids shaded left-diagonally were additionally open for exploratory fishing to that vessel from Sept. 3rd to Sept. 5th. A grey broken line marks the 52°S parallel delineating the boundary between north and south assessment sub-areas.

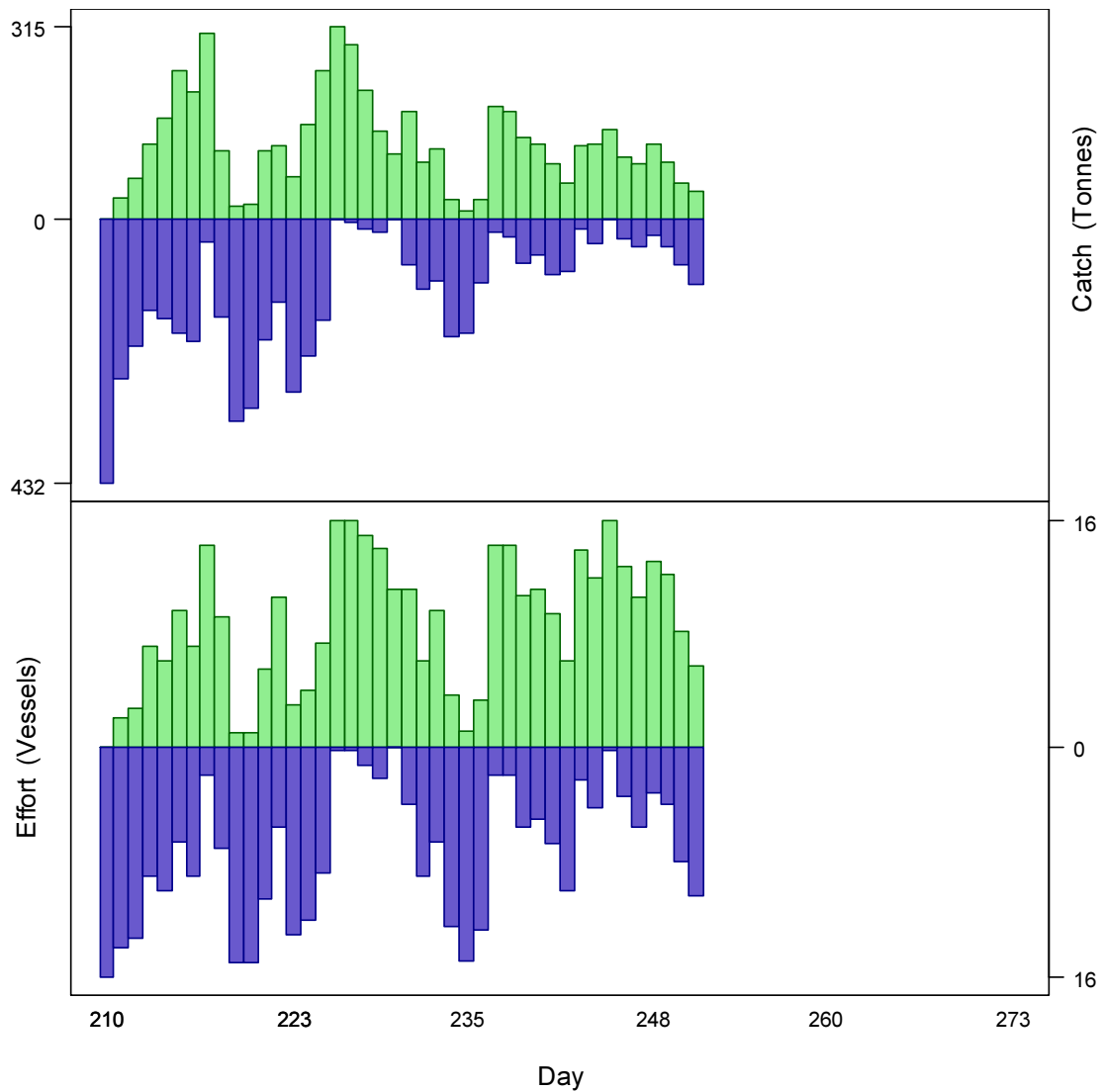


Figure 2. Daily total Falkland calamari catch and effort distribution by assessment sub-area north (green) and south (purple) of the 52° S parallel during 2nd season 2015. The season was open from July 29th (chronological day 210) to September 8th (chronological day 251). As many as 16 vessels fished per day north of 52° S; as many as 16 vessels fished per day south of 52° S. As much as 315 tonnes calamari was caught per day north of 52° S; as much as 432 tonnes calamari was caught per day south of 52° S.

Group arrivals / depletion criteria

Start days of depletions - following arrivals of new calamari groups - are judged primarily with reference to daily changes in CPUE, with additional information from sex proportions, maturity, and average individual sizes. The relationship of north-south to east-west wind speed vectors may differentiate between actual new arrivals of calamari groups and concentration of groups already present (Winter and Arkhipkin, 2015). CPUE is calculated as metric tonnes of calamari caught per vessel per day, i.e., days are used rather than trawl hours as the basic unit of effort. Commercial vessels do not trawl standardized duration hours, but rather durations that best suit their daily processing requirements. An effort index of days is therefore more consistent.

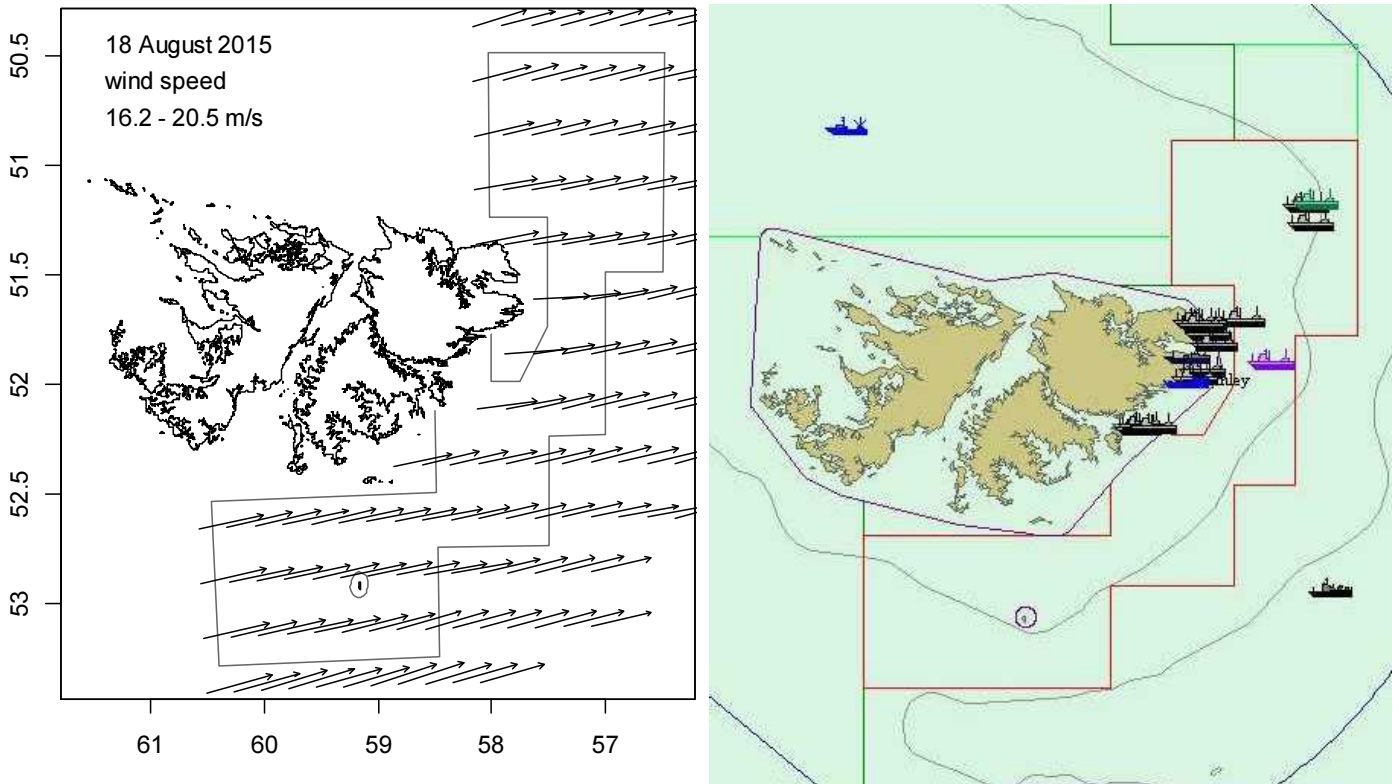
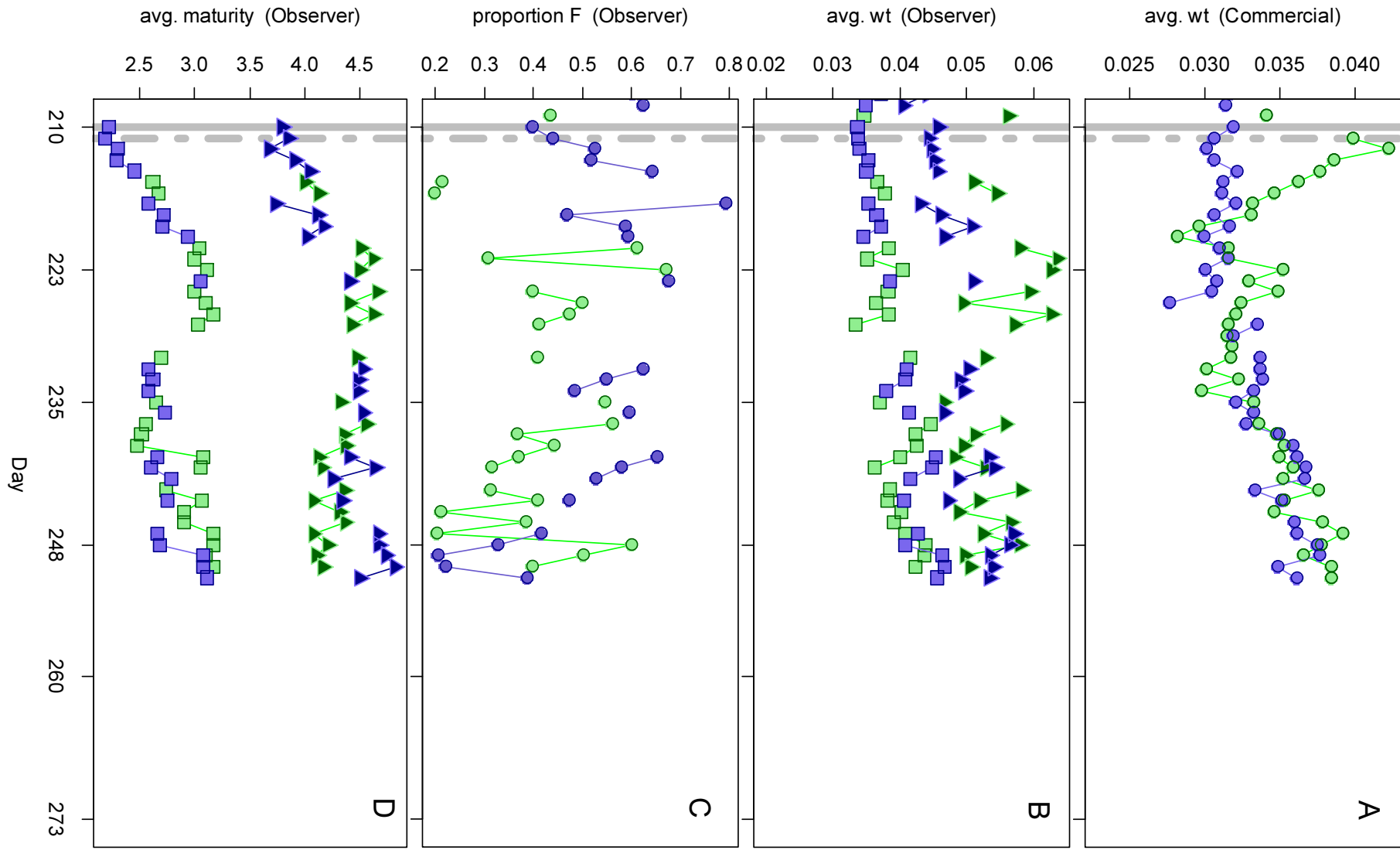


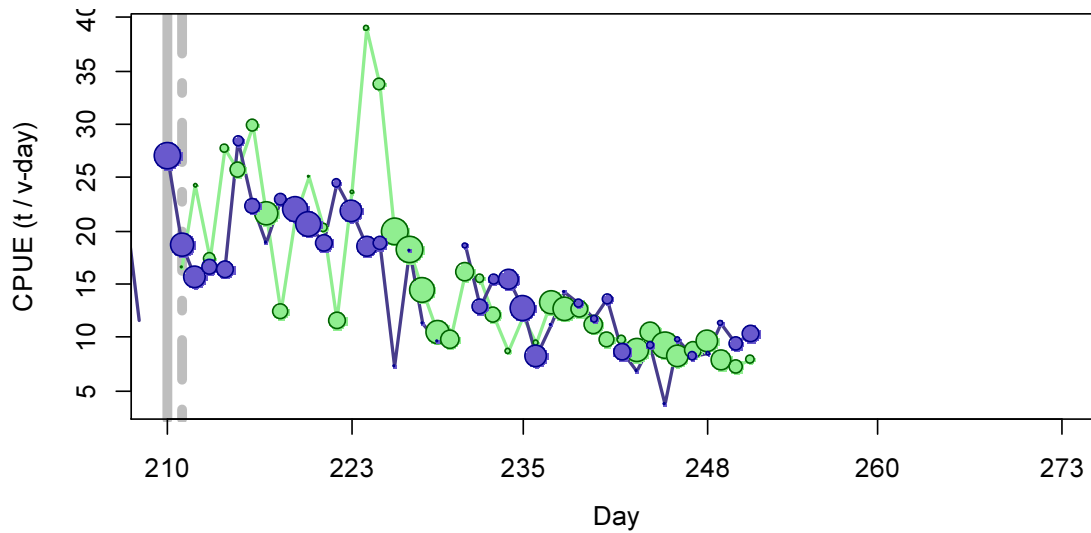
Figure 3. Left: wind speed vector plot at 0.25° resolution, from blended satellite observations (Zhang et al., 2006). Right: Fish Ops chart display. Both on August 18th when X-license fishing effort was reduced to less than a third of average because of weather conditions.

In this season, no further immigrations / depletions of calamari were recorded after the start of the commercial fishery. Sex proportions, maturities, and average individual sizes fluctuated throughout the season (Figure 4) but did not show trends related to important changes in CPUE. The decline in average commercial weights north over the first 10 days of the season was mostly from 2-3 vessels (Figure 4-A). Conversely, the high peak CPUE north on days 224-225 (12-13 August) (Figure 5) did not correspond to any decrease in sizes that would indicate younger, smaller squid entering the zone. It is always possible that small numbers of calamari ‘trickled’ in during the season, but the overall low levels of CPUE did not reveal such movements above the background variability. This is the first season since 2002 that did not record any in-season immigration.

Figure 4 [next page]. A: Average individual calamari weights (kg) per day from commercial size categories. B: Avg. individual weights (kg) by sex per day from observer sampling. C: Proportions of females / day from observer sampling. D: avg. maturity value by sex / day from observer sampling. All graphs – Males: triangles, females: squares, unsexed: circles. North sub-area: green, south sub-area: purple. Data from consecutive days are joined by line segments. Solid gray bars and broken gray bars indicate days 210 and 211, respectively the start of in-season depletions south and north.

Figure 5 [following page]. CPUE in metric tonnes per vessel per day, by assessment sub-area north (green) and south (purple) of the 52° S parallel. Circle sizes are proportioned to the numbers of vessel fishing. Data from consecutive days are joined by line segments. The solid gray bar and the broken gray bar indicate days 210 and 211, respectively the start of in-season depletions south and north.





Depletion analyses North

In the north sub-area, Bayesian optimization on catchability (q) resulted in a posterior (max. likelihood Bayesian $q_N = 1.636 \times 10^{-3}$; Figure 6, left, and Equation A9-N) that was closer to the pre-season prior (prior $q_N = 1.499 \times 10^{-3}$; Figure 6, left, and Equation A4-N) than to the in-season depletion (depletion $q_N = 2.180 \times 10^{-3}$; Figure 6, left, and A6-N). Respective weights in the Bayesian optimization (converse of the CVs) were 0.437 for the in-season depletion (A5-N) and 0.274 for the prior (A8-N).

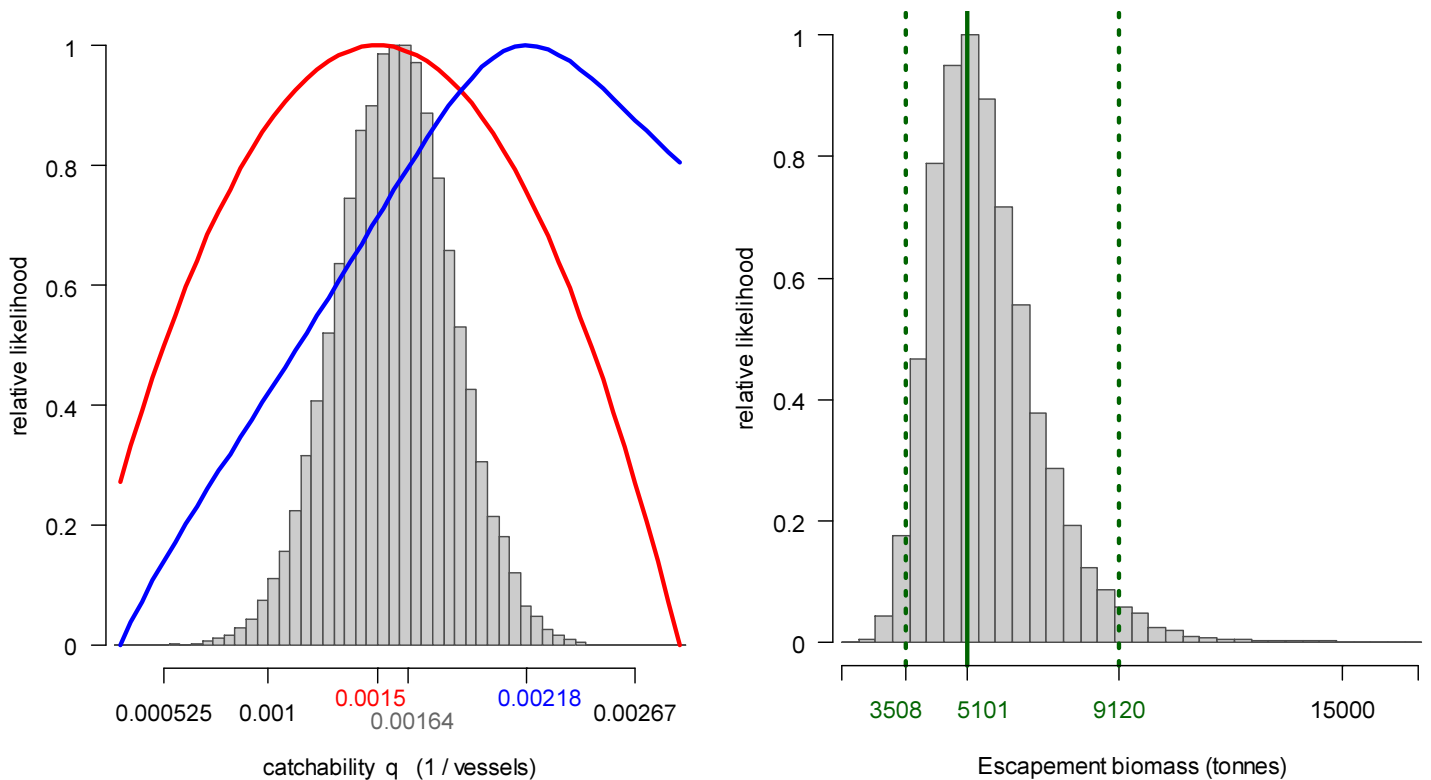


Figure 6 [previous page]. North sub-area. Left: Likelihood distributions for calamari catchability. Red line: prior model (pre-season survey data), blue line: in-season depletion model, gray bars: combined Bayesian model. Right: Likelihood distribution (gray bars) of escapement biomass, from Bayesian posterior and average individual calamari weight at the end of the season. Green lines: maximum likelihood and 95% confidence interval. Note the correspondence to Figure 7.

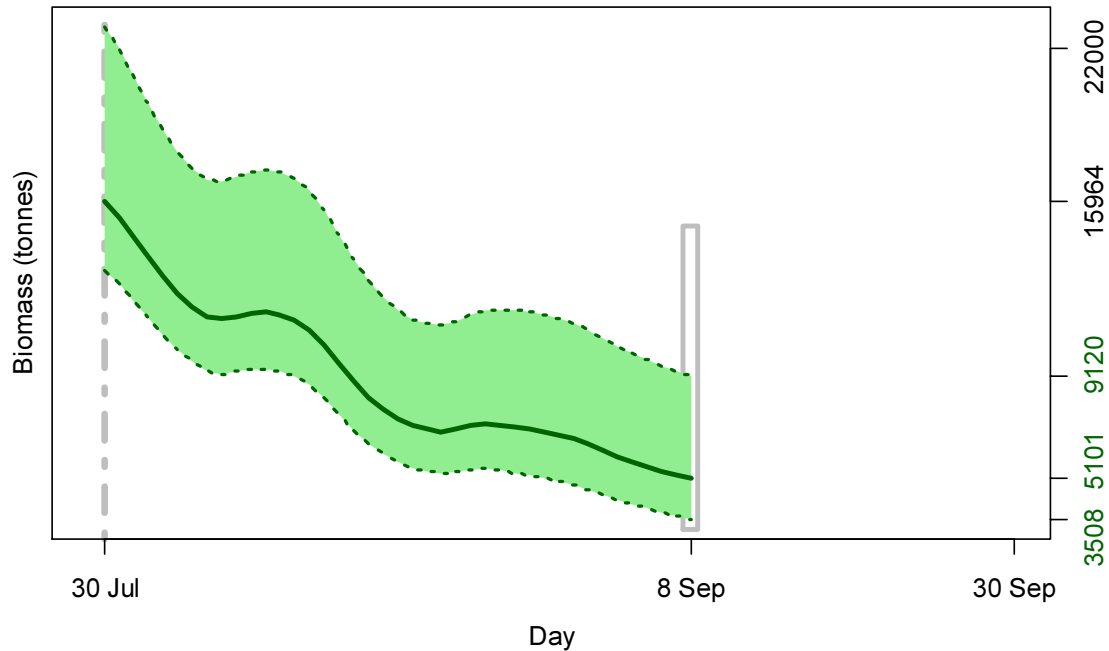


Figure 7. North sub-area. Calamari biomass time series estimated from Bayesian posterior of the depletion model \pm 95% confidence intervals. The broken gray bar indicates the start of in-season depletion north; July 30th (day 211). Note that the biomass ‘footprint’ on September 8th corresponds to the right-side plot of Figure 6.

The MCMC distribution of the Bayesian posterior multiplied by the GAM fit of average individual calamari weight (Figure A1-north) gave the likelihood distribution of calamari biomass on day 251 (September 8th) shown in Figure 6-right, with maximum likelihood and 95% confidence interval of:

$$B_{N \text{ day } 251} = 5,101 \text{ t} \sim 95\% \text{ CI } [3,508 - 9,120] \text{ t} \quad (8)$$

At its highest point (start of the season: day 211 - July 30th), estimated calamari biomass north was 15,964 t \sim 95% CI [13,236 – 22,847] t (Figure 7).

South

In the south sub-area, catchability coefficients (q) were slightly higher than the north: Bayesian posterior max. likelihood $q_S = 1.741 \times 10^{-3}$ (Figure 8, left, and equation A9-S), preseason prior $q_S = 1.620 \times 10^{-3}$ (Figure 8, left, and equation A4-S), and in-season depletion $q_S = 2.602 \times 10^{-3}$ (Figure 8, left, and A6-S). Bayesian optimization was weighted 0.600 for in-season depletion (A5-S) vs. 0.258 for the prior (A8-S).

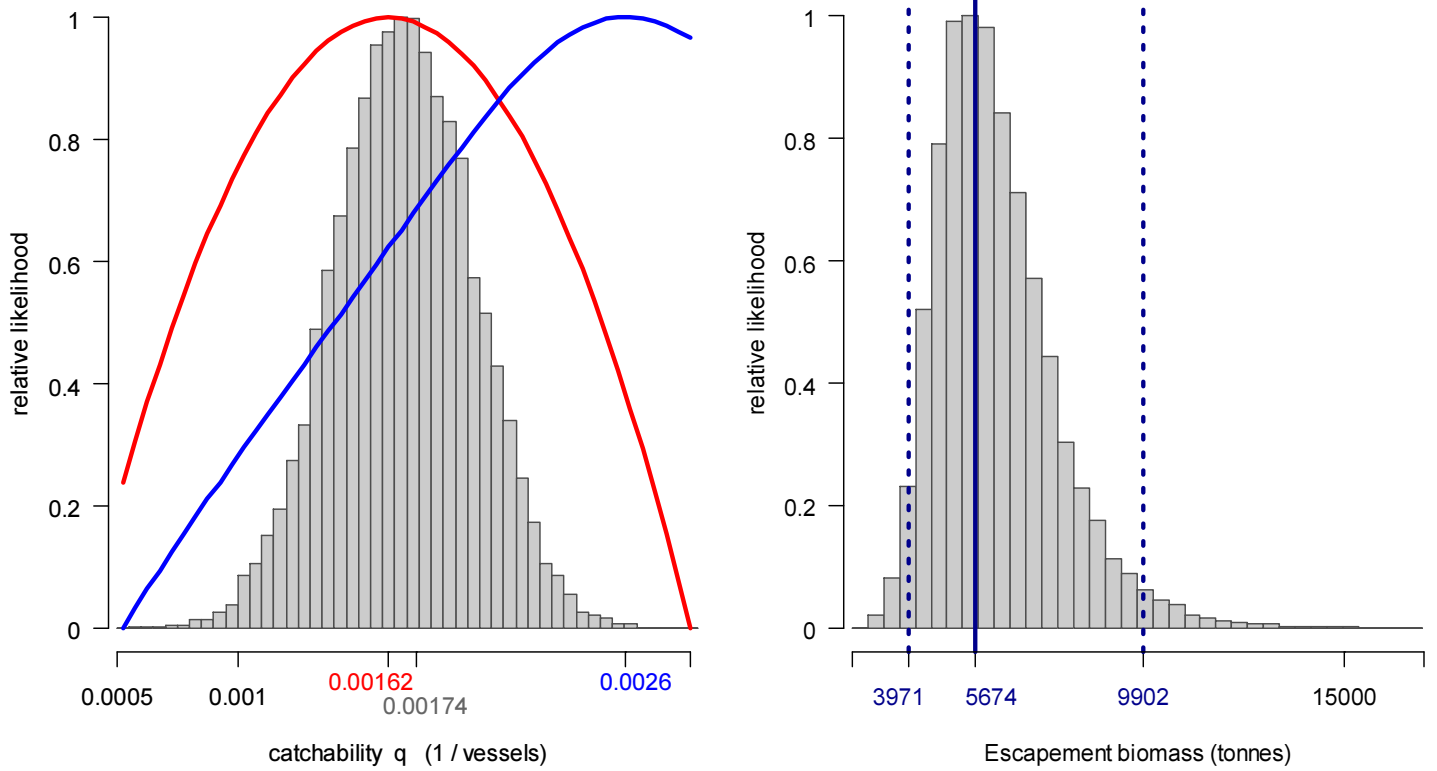


Figure 8. South sub-area. Left: Likelihood distributions for calamari catchability. Red line: prior model (pre-season survey data), blue line: in-season depletion model, gray bars: combined Bayesian model. Right: Likelihood distribution (gray bars) of escapement biomass, from Bayesian posterior and average individual calamari weight at the end of the season. Blue lines: maximum likelihood and 95% confidence interval. Note correspondence to Figure 9.

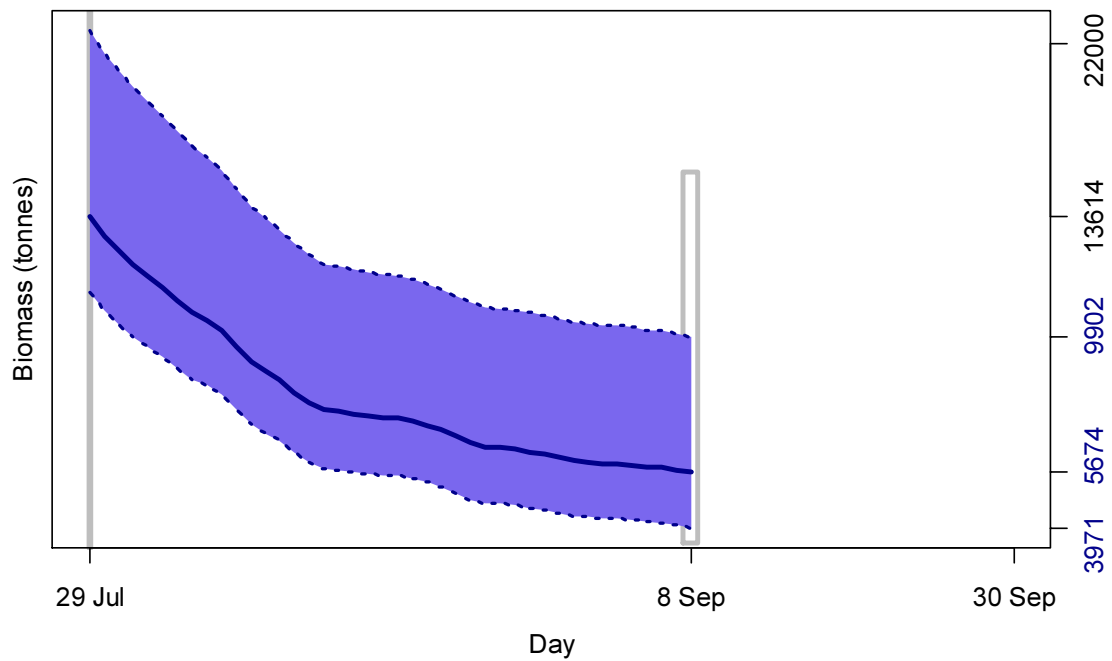


Figure 9 [previous page]. South sub-area. Calamari biomass time series estimated from Bayesian posterior of the depletion model \pm 95% confidence intervals. The broken gray bar indicates the start of in-season depletion north; July 29th (day 210). Note that the biomass ‘footprint’ on September 8th corresponds to the right-side plot of Figure 8.

The MCMC distribution of the Bayesian posterior multiplied by the GAM fit of average individual calamari weight (Figure A1-south) gave the likelihood distribution of calamari biomass on day 251 (September 8th) shown in Figure 8-right, with maximum likelihood and 95% confidence interval of:

$$B_{S \text{ day } 251} = 5,674 \text{ t} \sim 95\% \text{ CI } [3,971 - 9,902] \text{ t} \quad (9)$$

At its highest point (start of the season; July 29th), estimated calamari biomass south was 13,614 t \sim 95% CI [11,286 – 19,399] t (Figure 9).

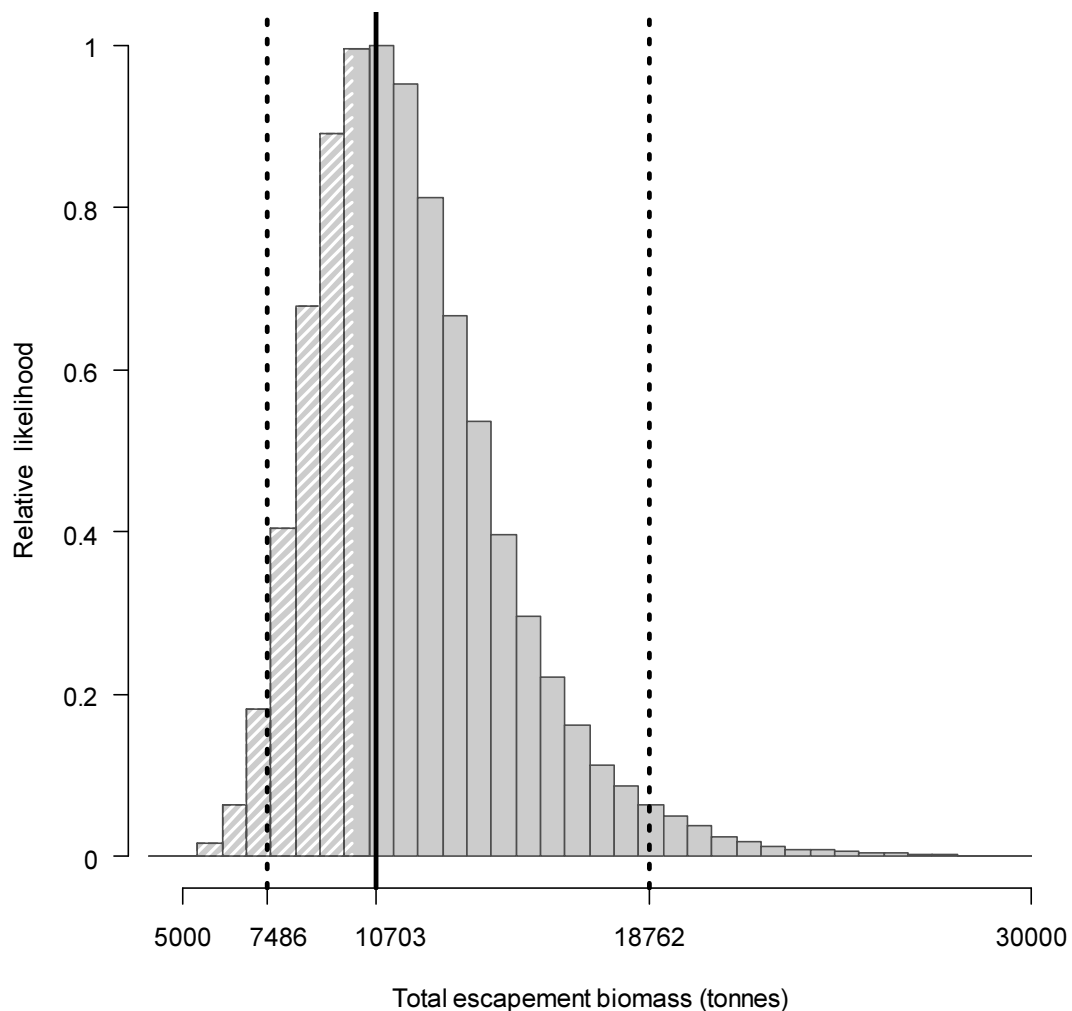


Figure 10. Likelihood distribution with 95% confidence intervals of total Falkland calamari escapement biomass at the end of the season (September 8th). White shading lines: portion of the distribution $<$ 10,000 tonnes; equal to 29.0% of the whole distribution.

Escapement biomass

Total escapement biomass was defined as the aggregate biomass of Falkland calamari at the end of day 251 (September 8th) for north and south sub-areas combined (equations 8 and 9). Depletion models are calculated on the inference that all fishing and natural mortality are gathered at mid-day, thus a half day of mortality ($e^{-M/2}$) was added to correspond to the closure of the fishery at 23:59 (mid-night) on September 8th: equation 10. Semi-randomized addition of the north and south biomass estimates gave the aggregate likelihood distribution of total escapement biomass shown in Figure 10.

$$\begin{aligned} B_{\text{Total day 251}} &= (B_{\text{N day 251}} + B_{\text{S day 251}}) \times e^{-M/2} \\ &= 10,703 \text{ t} \sim 95\% \text{ CI } [7,486 - 18,762] \text{ t} \end{aligned} \quad (10)$$

The risk of the fishery, defined as the proportion of the total escapement biomass distribution below the conservation limit of 10,000 tonnes (Agnew et al., 2002; 2005; Barton, 2002), was calculated as 29.0% (Figure 10). The National Standard Guidelines of NOAA Fisheries recommend that actual catch should not exceed annual catch limits of a fishery more than once over a 4-year period (Patrick et al., 2013). While this ‘1 in 4’ standard is not per se computationally equivalent to a 25% risk, it can be taken as a comparative approximation. Thus, the maximum likelihood escapement of 10,703 tonnes was above the conservation threshold, but in relation to the uncertainty of estimation by a margin that should be considered about minimal.

Mortality / Emigration

As this season – uncommonly – did not include immigrations, the depletion model structures were relatively simple and provided an opportunity to examine the assumed natural mortality rate. In all recent stock assessments, natural mortality has been assigned the fixed instantaneous rate of 0.01333 day^{-1} (Roa-Ureta and Arkhipkin, 2007), based on the maximum observed *D. gahi* age of 352 days (FIFD data) applied to Hewitt and Hoenig’s (2005) empirical equation:

$$\log(M) = 1.44 - 0.982 \times \log(352 \text{ days}) \quad (11)$$

Alternatively, mortality could be set as a free parameter in the optimization of the depletion model. This alternative was tested for this season, using 0.01333 day^{-1} as the starting value in the optimizations and treating the algorithms (equations 1 to 6) the same in all other respects. The optimizations resulted in higher values of M and corresponding slightly lower maximum likelihood estimates of escapement biomass:

$$\begin{aligned} \text{opt. } M_{\text{North}} &= 0.01851 \text{ day}^{-1} \\ B_{\text{N day 251 (opt. M)}} &= 5,058 \text{ t} \end{aligned} \quad (12\text{-N})$$

$$\begin{aligned} \text{opt. } M_{\text{South}} &= 0.02065 \text{ day}^{-1} \\ B_{\text{S day 251 (opt. M)}} &= 5,401 \text{ t} \end{aligned} \quad (12\text{-S})$$

Confidence intervals were not calculated for this exercise.

Roa-Ureta (2012) implemented free-parameter M optimization, and found M values significantly lower than 0.01333 day^{-1} . Roa-Ureta (2012) reasoned that mortality rates during

the fishing season would be lower than the lifespan average, because fishing seasons end before the period of biologically determined post-spawning death. To have instead obtained higher M values (equations 12) than the empirical estimate (equation 11) suggests that these M values include emigration. Calamari enter the fishing zone to feed and grow, then return to the inshore spawning grounds upon maturity (Arkhipkin and Middleton, 2002; Arkhipkin et al., 2008). The bulk of that emigration occurs after the end of the season (indeed, the season is timed for it), but in concert with squid immigrating at intervals within the season (Roa-Ureta, 2012; Winter and Arkhipkin, 2015), some in-season emigration should be expected. A few calamari may also move outward into deeper water beyond the fishing grounds. Taking the difference between total optimized mortality (equations 12) and net empirical mortality (equation 11) gives putative emigration rates of:

$$\text{Emigration Prop. N} = 1 - e^{(0.01851 - 0.01333)} = 0.5\% \text{ day}^{-1} \quad (13-N)$$

$$\text{Emigration Prop. S} = 1 - e^{(0.02065 - 0.01333)} = 0.7\% \text{ day}^{-1} \quad (13-S)$$

These calculations should be considered preliminary. The depletion model (DeLury, 1947) is based on the principle that removals from the population are observed data, not model inferences. Roa-Ureta (2012), for example, obtained unrealistically high inter-annual variations of optimized M . The approach of modelling natural mortality may however provide useful information with further testing.

Evaluation of season schedule change

The scheduling change of delaying the 2nd season opening by one further week would normally call for evaluation of the outcome to the Falkland calamari stock. In this season however, the outcome cannot be discriminated from the effects of the unusual presence of *Illex* earlier in the year (Winter, 2015), and the consequent emergency closure of 2nd season. Therefore, evaluation of the season schedule change will be deferred until next year.

Fishing outside the Loligo Box

With low catches in the Loligo Box, vessel operators requested access to adjoining areas. The Director of Fisheries authorized opening of grid XVAM from September 1st for the rest of the season, exploratory opening of grids XKAM, XKAN, XKAP, XJAN and XJAP for one vessel with observer from September 1st to September 3rd, and additional exploratory opening of grids XHAL, XHAM, XHAN and XJAM for the same vessel with observer from September 3rd to September 5th (Figure 1).

Grid XVAM was never fished. The grids north of the Loligo Box were fished by the exploratory vessel for 16 trawls from September 1st to September 4th. Following the procedure used last year (Winter, 2014), the exploratory catches were compared to the average of vessels fishing in the top three ‘rows’ of the Loligo Box (between 50.5° S and 51.25° S) on the same days plus one day before and after. These data are shown in Table 2. To avoid identifying the exploratory vessel’s catches outright, data are standardized to “1” as the maximum single-day calamari catch.

Over the 4 days of exploratory fishing, the vessel north of the Loligo Box averaged higher calamari catch for the first two days, then lower calamari catch for the next two days, compared to vessels inside the north of the Loligo Box. Concurrently the vessel north of the Loligo Box averaged lower rock cod bycatch (*Patagonotothen ramsayi*) for the first two

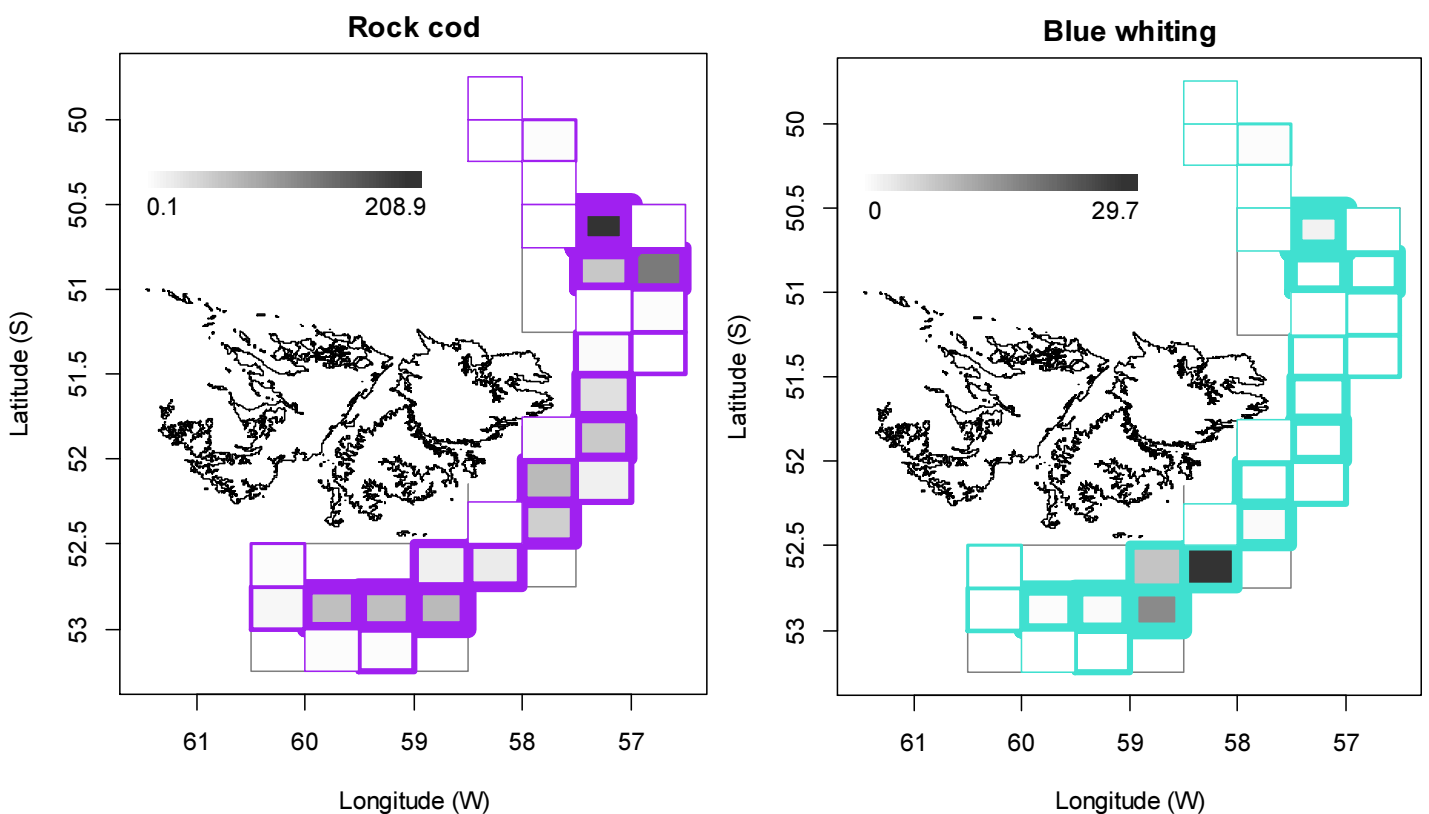
days, then higher rock cod bycatch for the next two days. Other bycatch was consistently higher north of the Loligo Box but low overall (Table 2).

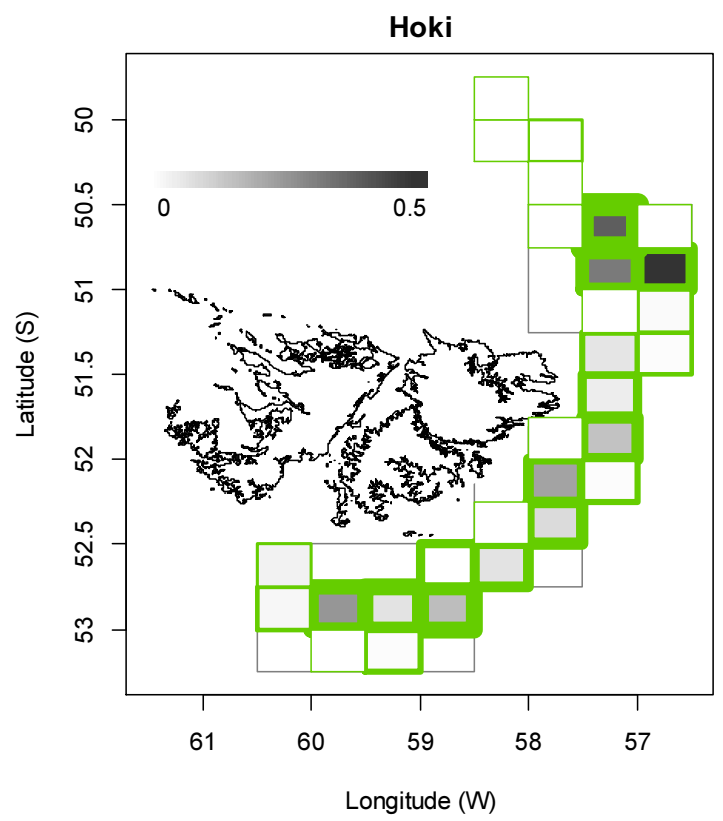
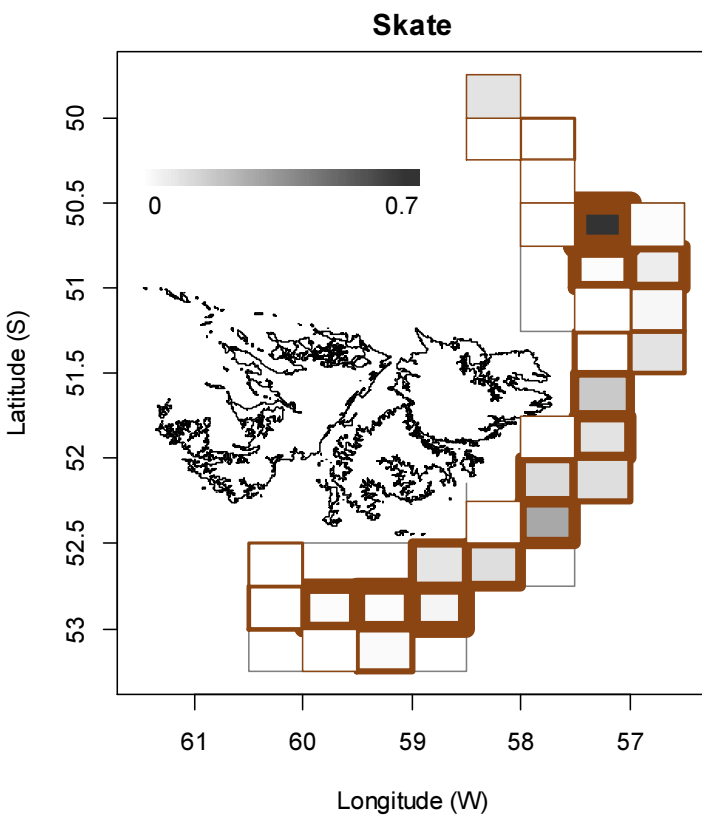
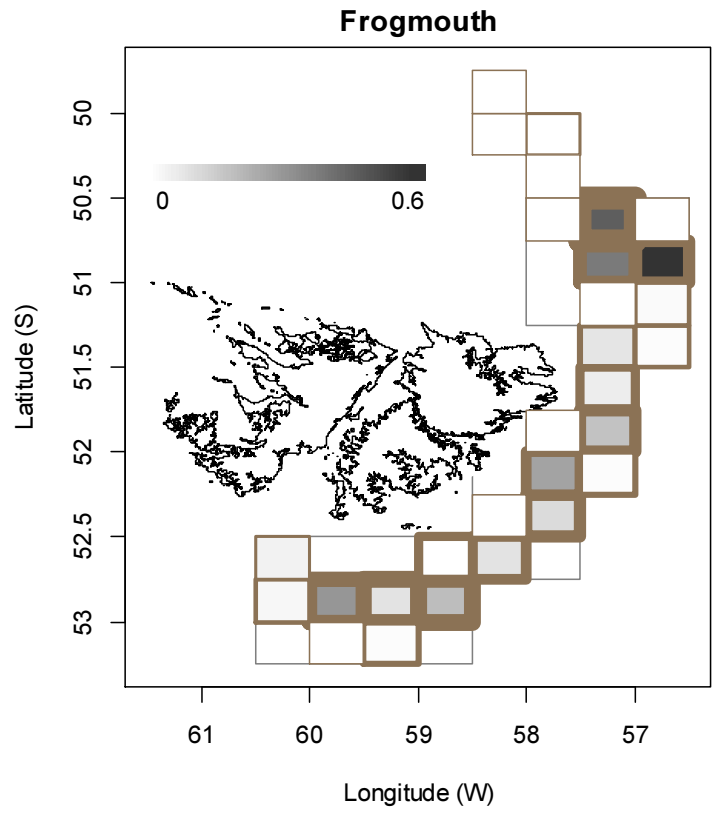
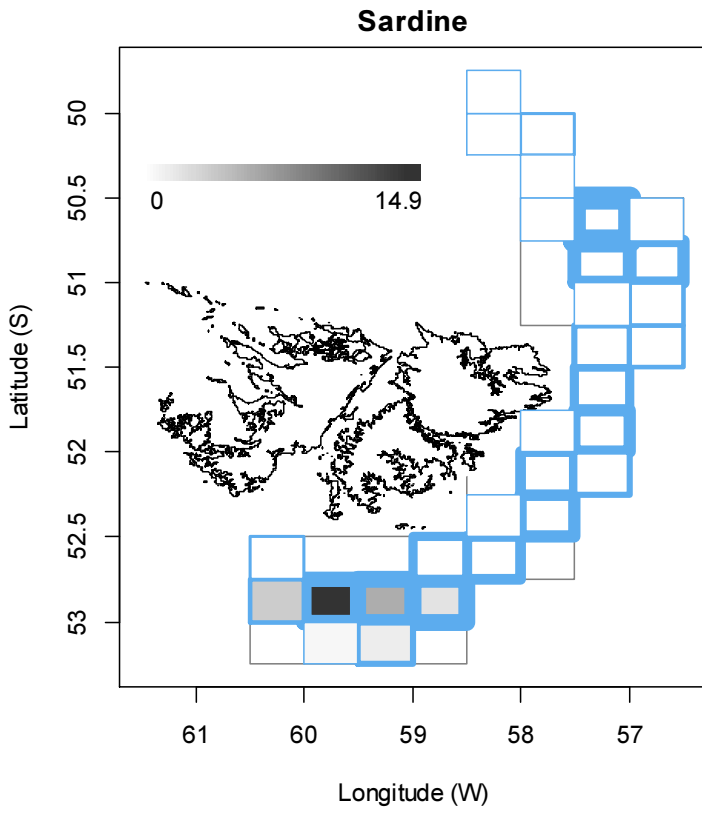
Table 2. Proportional catches (max. = 1) of calamari (LOL), rock cod (PAR) and other bycatch of the X-licensed vessel permitted to fish north of the Loligo Box, compared to vessels (N = number per day) that fished by regular license statute in the northern part of the Loligo Box over the same range of days.

Date	Vessel North of Box				Vessels inside North Box			
	N	LOL	PAR	Other Bycatch	N	LOL	PAR	Other Bycatch
31/08	0	-	-	-	5.9	0.725	0.148	0.001
01/09	1	0.924	0.038	0.015	9.2	0.765	0.080	0.000
02/09	1	1.000	0.021	0.007	14.0	0.651	0.121	0.004
03/09	1	0.450	0.081	0.067	7.0	0.596	0.064	0.005
04/09	0.7	0.546	0.106	0.041	7.3	0.627	0.057	0.000
05/09	0	-	-	-	11.5	0.689	0.086	0.002
Avg.		0.747	0.057	0.032		0.676	0.094	0.002

Bycatch

Figure 11 [below]. Distributions of the six principal bycatches during 2nd season 2015. Thickness of grid lines is proportional to the number of vessel-days (1 to 239). Gray-scale is proportional to the bycatch biomass; maximum indicated on each plot.





Of the 665 vessel-days in total (Table 1), 4 vessel-days reported a catch of more rock cod than calamari; all four within the last week of the season. The most common bycatches reported overall for the season were rock cod (894 t, reported from 621 vessel-days), blue whiting (*Micromesistius australis*) (60 t, 88 vessel-days), sardine (*Sprattus fuegensis*) (28 t, 49 vessel-days), frogmouth (*Cottoperca gobio*) (3 t, 46 vessel-days), skates (Rajidae) (2 t, 68 vessel-days), and hoki (*Macruronus magellanicus*) (0.8 t, 12 vessel-days). Relative distributions of these bycatches are shown in Figure 11.

References

- Agnew, D.J., Baranowski, R., Beddington, J.R., des Clers, S., Nolan, C.P. 1998. Approaches to assessing stocks of *Loligo gahi* around the Falkland Islands. *Fisheries Research* 35:155-169.
- Agnew, D. J., Beddington, J. R., and Hill, S. 2002. The potential use of environmental information to manage squid stocks. *Canadian Journal of Fisheries and Aquatic Sciences*, 59: 1851–1857.
- Agnew, D.J., Hill, S.L., Beddington, J.R., Purchase, L.V., Wakeford, R.C. 2005. Sustainability and management of Southwest Atlantic squid fisheries. *Bulletin of Marine Science* 76: 579-593.
- Arkhipkin, A.I., Middleton, D.A.J. 2002. Sexual segregation in ontogenetic migrations by the squid *Loligo gahi* around the Falkland Islands. *Bulletin of Marine Science* 71: 109-127.
- Arkhipkin, A.I., Middleton, D.A.J., Barton, J. 2008. Management and conservation of a short-lived fishery resource: *Loligo gahi* around the Falkland Islands. *American Fisheries Society Symposium* 49:1243-1252.
- Barton, J. 2002. Fisheries and fisheries management in Falkland Islands Conservation Zones. *Aquatic Conservation: Marine and Freshwater Ecosystems*, 12: 127–135.
- Boag, T. 2015. Observer Report 1066. Technical Document, FIG Fisheries Department. 26 p.
- Brooks, S.P., Gelman, A. 1998. General methods for monitoring convergence of iterative simulations. *Journal of computational and graphical statistics* 7:434-455.
- DeLury, D.B. 1947. On the estimation of biological populations. *Biometrics* 3:145-167.
- Fisheries Committee. 2013. Re-allocation of fishing effort between 1st and 2nd *Loligo* seasons. Proposal to the Fisheries Committee, December 2013. 4 p.
- Gamerman, D., Lopes, H.F. 2006. Markov Chain Monte Carlo. Stochastic simulation for Bayesian inference. 2nd edition. Chapman & Hall/CRC.
- Hewitt, D.A., Hoenig, J.M. 2005. Comparison of two approaches for estimating natural mortality based on longevity. *Fishery Bulletin* 103: 433-437.
- Jones, J. 2015. Observer Report 1068. Technical Document, FIG Fisheries Department. 27 p.
- Jones, J., Winter, A., Shcherbich, Z., Boag, T. 2015. *Loligo* stock assessment survey, 2nd season 2014. Technical Document, Falkland Islands Fisheries Department. 18 p.
- Jürgens, L. 2015. Observer Report 1069. Technical Document, FIG Fisheries Department. 20 p.

- Magnusson, A., Punt, A., Hilborn, R. 2013. Measuring uncertainty in fisheries stock assessment: the delta method, bootstrap, and MCMC. *Fish and Fisheries* 14: 325-342.
- Nash, J.C., Varadhan, R. 2011. optimx: A replacement and extension of the optim() function. R package version 2011-2.27. <http://CRAN.R-project.org/package=optimx>
- Patrick, W.S., Morrison, W., Nelson, M., González Marrero, R.L. 2013. Factors affecting management uncertainty in U.S. fisheries and methodological solutions. *Ocean & Coastal Management* 71: 64-72.
- Patterson, K.R. 1988. Life history of Patagonian squid *Loligo gahi* and growth parameter estimates using least-squares fits to linear and von Bertalanffy models. *Marine Ecology Progress Series* 47:65-74.
- Payá, I. 2010. Fishery Report. *Loligo gahi*, Second Season 2009. Fishery statistics, biological trends, stock assessment and risk analysis. Technical Document, Falkland Islands Fisheries Department. 54 p.
- Punt, A.E., Hilborn, R. 1997. Fisheries stock assessment and decision analysis: the Bayesian approach. *Reviews in Fish Biology and Fisheries* 7:35-63.
- Roa-Ureta, R. 2012. Modelling in-season pulses of recruitment and hyperstability-hyperdepletion in the *Loligo gahi* fishery around the Falkland Islands with generalized depletion models. *ICES Journal of Marine Science*, 69: 1403–1415.
- Roa-Ureta, R., Arkhipkin, A.I. 2007. Short-term stock assessment of *Loligo gahi* at the Falkland Islands: sequential use of stochastic biomass projection and stock depletion models. *ICES Journal of Marine Science* 64:3-17.
- Rosenberg, A.A., Kirkwood, G.P., Crombie, J.A., Beddington, J.R. 1990. The assessment of stocks of annual squid species. *Fisheries Research* 8:335-350.
- Shaw, P.W., Arkhipkin, A.I., Adcock, G.J., Burnett, W.J., Carvalho, G.R., Scherbich, J.N., Villegas, P.A. 2004. DNA markers indicate that distinct spawning cohorts and aggregations of Patagonian squid, *Loligo gahi*, do not represent genetically discrete subpopulations. *Marine Biology* 144: 961-970.
- Winter, A., Arkhipkin, A. 2015. Environmental impacts on recruitment migrations of Patagonian longfin squid (*Doryteuthis gahi*) in the Falkland Islands with reference to stock assessment. *Fisheries Research* 172: 85-95.
- Winter, A. 2014. *Loligo* stock assessment, second season 2014. Technical Document, Falkland Islands Fisheries Department. 28 p.
- Winter, A. 2015. *Loligo* stock assessment, first season 2015. Technical Document, Falkland Islands Fisheries Department. 28 p.
- Zhang, H.-M., Bates, J.J., Reynolds, R.W. 2006. Assessment of composite global sampling: Sea surface wind speed. *Geophysical Research Letters* 33: L17714.

Appendix

Falkland calamari individual weights

A generalized additive model (GAM) was calculated from the daily observer data (both sexes combined) and commercial size category data of average individual daily weights of calamari. North and south sub-areas were calculated separately. For continuity, the GAMs were calculated using all pre-season survey and in-season data contiguously. GAM plots of the north and south sub-areas are shown in Figure A1.

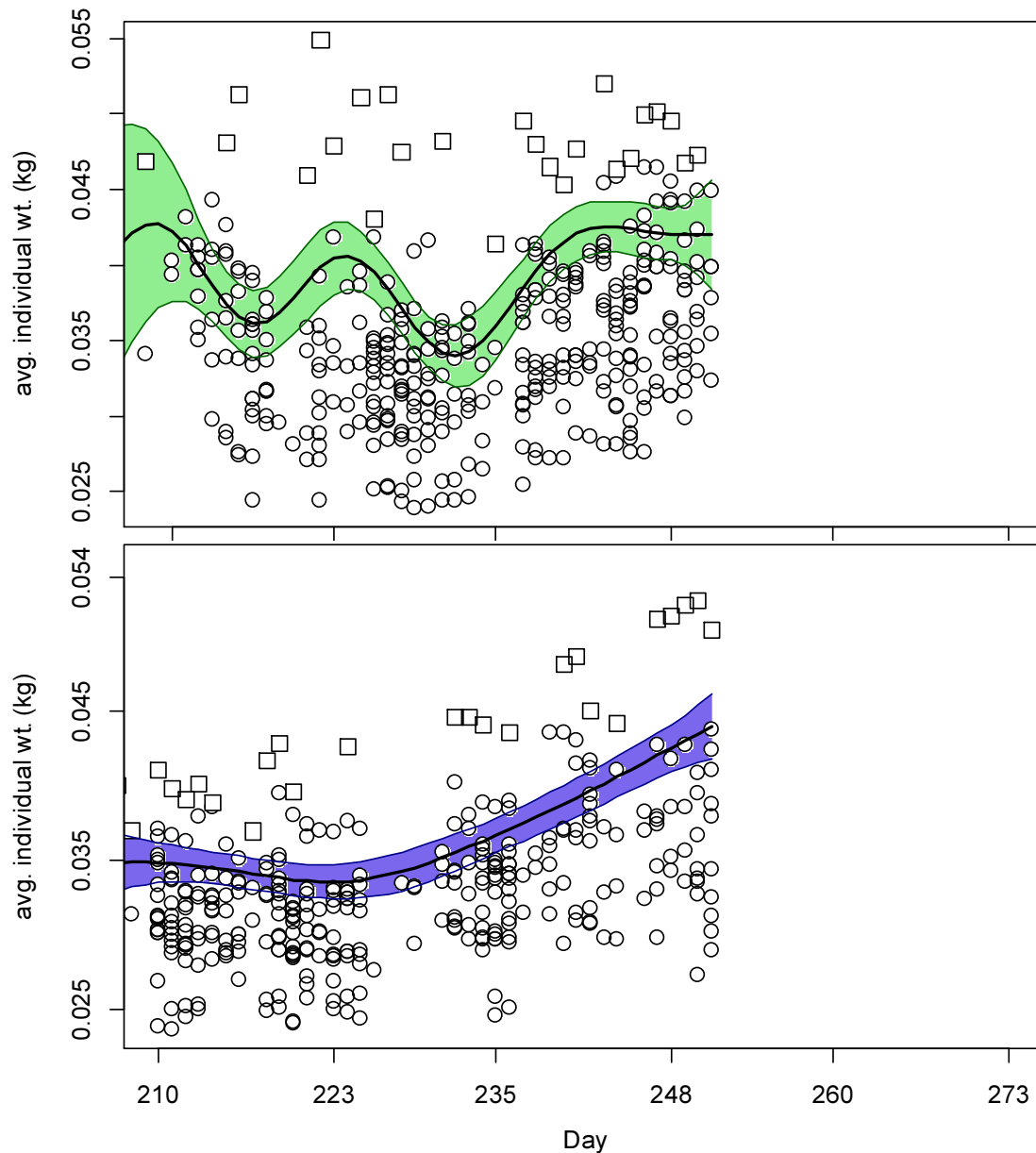


Figure A1. North (top) and south (bottom) sub-area daily average individual calamari weights from commercial size categories per vessel (circles) and observer measurements (squares). GAMs of the daily trends \pm 95% confidence intervals (centre lines and colour under-shading).

Prior estimates and CV

The pre-season survey (Jones et al., 2015) had estimated Falkland calamari biomasses of 9,014 t (standard deviation: $\pm 1,364$ t) north of 52° S and 16,407 t (standard deviation: $\pm 1,853$ t) south of 52° S. From modelled survey catchability, Payá (2010) had estimated average net escapement of up to 22%, which was added to the standard deviation:

$$9,014 \pm \left(\frac{1,364}{9,014} + .22 \right) = 9,014 \pm 37.1\% = 9,014 \pm 3,347 \text{ t} \quad (\text{A1-N})$$

$$16,407 \pm \left(\frac{1,853}{16,407} + .22 \right) = 16,407 \pm 33.3\% = 16,407 \pm 5,463 \text{ t} \quad (\text{A1-S})$$

The 22% was added as a linear increase in the variability, but was not used to reduce the total estimate, because calamari that escape one trawl are likely to be part of the biomass concentration that is available to the next trawl. This estimate in biomass was converted to an estimate in numbers using the size-frequency distributions sampled during the pre-season survey (Jones et al., 2015).

Calamari numbers at the start of the season, day 210, were estimated as the survey biomass estimates divided by the GAM-predicted individual weight averages for the survey: 0.034 kg north and 0.035 kg south. Coefficients of variation (CV) of the GAM were 11.1% north and 3.8% south, and CV of the length-weight conversion relationship (equation 7) were 6.4% north and 7.4% south. Combining all sources of variation with the pre-season survey biomass estimates and individual weight averages gave estimated calamari numbers at season start (July 29th, day 210) of:

$$\begin{aligned} \text{prior } N_{N \text{ day } 210} &= \frac{9,014 \times 1000}{0.034} \pm \sqrt{37.1\%^2 + 11.1\%^2 + 6.4\%^2} \\ &= 0.265 \times 10^9 \pm 39.3\% = 0.265 \times 10^9 \pm 0.104 \times 10^9 \end{aligned} \quad (\text{A2-N})$$

$$\begin{aligned} \text{prior } N_{S \text{ day } 210} &= \frac{16,407 \times 1000}{0.035} \pm \sqrt{33.3\%^2 + 3.8\%^2 + 7.4\%^2} \\ &= 0.479 \times 10^9 \pm 34.3\% = 0.478 \times 10^9 \pm 0.164 \times 10^9 \end{aligned} \quad (\text{A2-S})$$

The catchability coefficient (q) prior for the north sub-area was taken on day 211, the first day in the season that any fishing effort was taken in the north; by 2 vessels. The abundance (N) on day 211 was calculated as the abundance on start day 210 discounted for 1 day of only natural mortality (given that zero catch had been taken the day before):

$$\text{prior } N_{N \text{ day } 211} = \text{prior } N_{N \text{ day } 210} \times e^{-M \cdot (211-210)} = 0.262 \times 10^9 \quad (\text{A3-N})$$

$$\begin{aligned} \text{prior } q_N &= C(N)_{N \text{ day } 211} / (\text{prior } N_{N \text{ day } 211} \times E_{N \text{ day } 211}) \\ &= (C(B)_{N \text{ day } 211} / Wt_{N \text{ day } 211}) / (\text{prior } N_{N \text{ day } 211} \times E_{N \text{ day } 211}) \\ &= (33.1 \text{ t} / 0.042 \text{ kg}) / (0.262 \times 10^9 \times 2 \text{ vessel-days}) \end{aligned}$$

$$= 1.499 \times 10^{-3} \text{ vessels}^{-1A} \quad (\text{A4-N})$$

The catchability coefficient prior for the south sub-area was taken on day 210, the first day of the season, when all 16 vessels were fishing south. As this was the first scheduled day of the season, no discount was applicable for either natural mortality or catch.

$$\begin{aligned} \text{prior } q_S &= C(N)_{S \text{ day } 210} / (\text{prior } N_{S \text{ day } 210} \times E_{S \text{ day } 210}) \\ &= (C(B)_{S \text{ day } 210} / Wt_{S \text{ day } 210}) / (\text{prior } N_{S \text{ day } 210} \times E_{S \text{ day } 210}) \\ &= (432.1 \text{ t} / 0.035 \text{ kg}) / (0.479 \times 10^9 \times 16 \text{ vessel-days}) \\ &= 1.620 \times 10^{-3} \text{ vessels}^{-1B} \end{aligned} \quad (\text{A4-S})$$

CVs of the priors were calculated as the sums of variability in $\text{prior } N$ (equations A2) plus variability in the catches of vessels on the q days (day 210 N and day 211 S):

$$\begin{aligned} CV_{\text{prior } N} &= \sqrt{39.3\%^2 + \left(\frac{SD(C(B)_{N \text{ vessels day } 211})}{\text{mean}(C(B)_{N \text{ vessels day } 211})} \right)^2} \\ &= \sqrt{39.3\%^2 + 18.0\%^2} = 43.7\% \end{aligned} \quad (\text{A5-N})$$

$$\begin{aligned} CV_{\text{prior } S} &= \sqrt{34.3\%^2 + \left(\frac{SD(C(B)_{S \text{ vessels day } 210})}{\text{mean}(C(B)_{S \text{ vessels day } 210})} \right)^2} \\ &= \sqrt{34.3\%^2 + 29.9\%^2} = 45.5\% \end{aligned} \quad (\text{A5-S})$$

Depletion model estimates and CV

For the north sub-area, the equivalent of equation 2 with one N_{day} was optimized on the difference between predicted and actual catches (equation 3), resulting in parameter values:

$$\begin{aligned} \text{depletion } N_{1N \text{ day } 211} &= 0.310 \times 10^9 \\ \text{depletion } q_N &= 2.180 \times 10^{-3} \text{ vessels}^{-1A} \end{aligned} \quad (\text{A6-N})$$

The root-mean-square deviation of predicted vs. actual catches was calculated and divided by the mean actual catch to measure fit of the optimization:

$$\begin{aligned} CV_{\text{rmsd } N} &= \frac{\sqrt{\sum_i (\text{predicted } C(N)_{N \text{ day } i} - \text{actual } C(N)_{N \text{ day } i})^2}}{\text{mean}(\text{actual } C(N)_{N \text{ day } i})} \\ &= 8.909 \times 10^5 / 3.266 \times 10^6 = 27.3\% \end{aligned} \quad (\text{A7-N})$$

^A On Figure 6-left.

^B On Figure 8-left.

$CV_{\text{rmsd N}}$ was added to the variability of the GAM-predicted individual weight averages for the season (Figure A1-N); equal to a CV of 3.0% north. CVs of the depletion were then calculated as the sum:

$$\begin{aligned} CV_{\text{depletion N}} &= \sqrt{CV_{\text{rmsd N}}^2 + CV_{\text{GAM Wt N}}^2} = \sqrt{27.3\%^2 + 3.0\%^2} \\ &= 27.4\% \end{aligned} \quad (\text{A8-N})$$

For the south sub-area, the equivalent of equation 2 with one N_{day} was optimized on the difference between predicted and actual catches (equation 3), resulting in parameter values:

$$\begin{aligned} \text{depletion } N_{1S \text{ day } 210} &= 0.302 \times 10^9 \\ \text{depletion } Q_S &= 2.602 \times 10^{-3} \text{ vessels}^{-1B} \end{aligned} \quad (\text{A6-S})$$

The root-mean-square deviation of predicted vs. actual catches was calculated and divided by the mean actual catch to measure fit of the optimization:

$$\begin{aligned} CV_{\text{rmsd S}} &= \frac{\sqrt{\sum_i (\text{predicted } C(N)_{S \text{ day } i} - \text{actual } C(N)_{S \text{ day } i})^2}}{\text{mean}(\text{actual } C(N)_{S \text{ day } i})} \\ &= 1.076 \times 10^6 / 3.459 \times 10^6 = 31.1\% \end{aligned} \quad (\text{A7-S})$$

$CV_{\text{rmsd S}}$ was added to the variability of the GAM-predicted individual weight averages for the season (Figure A1-S); equal to a CV of 1.7% south. CVs of the depletion were then calculated as the sum:

$$\begin{aligned} CV_{\text{depletion S}} &= \sqrt{CV_{\text{rmsd S}}^2 + CV_{\text{GAM Wt S}}^2} = \sqrt{31.1\%^2 + 1.7\%^2} \\ &= 31.1\% \end{aligned} \quad (\text{A8-S})$$

Combined Bayesian models

For the north sub-area, joint optimization of equations 3 and 4 resulted in parameter values:

$$\begin{aligned} \text{depletion } N_{1N \text{ day } 211} &= 0.378 \times 10^9 \\ \text{depletion } Q_N &= 1.636 \times 10^{-3} \text{ vessels}^{-1A} \end{aligned} \quad (\text{A9-N})$$

These parameters produced the fit between predicted and actual catches shown in Fig. A2-N.

For the south sub-area, joint optimization of equations 3 and 4 resulted in parameter values:

$$\begin{aligned} \text{depletion } N_{1S \text{ day } 211} &= 0.391 \times 10^9 \\ \text{depletion } Q_S &= 1.741 \times 10^{-3} \text{ vessels}^{-1B} \end{aligned} \quad (\text{A9-S})$$

These parameters produced the fit between predicted and actual catches shown in Fig. A2-S.

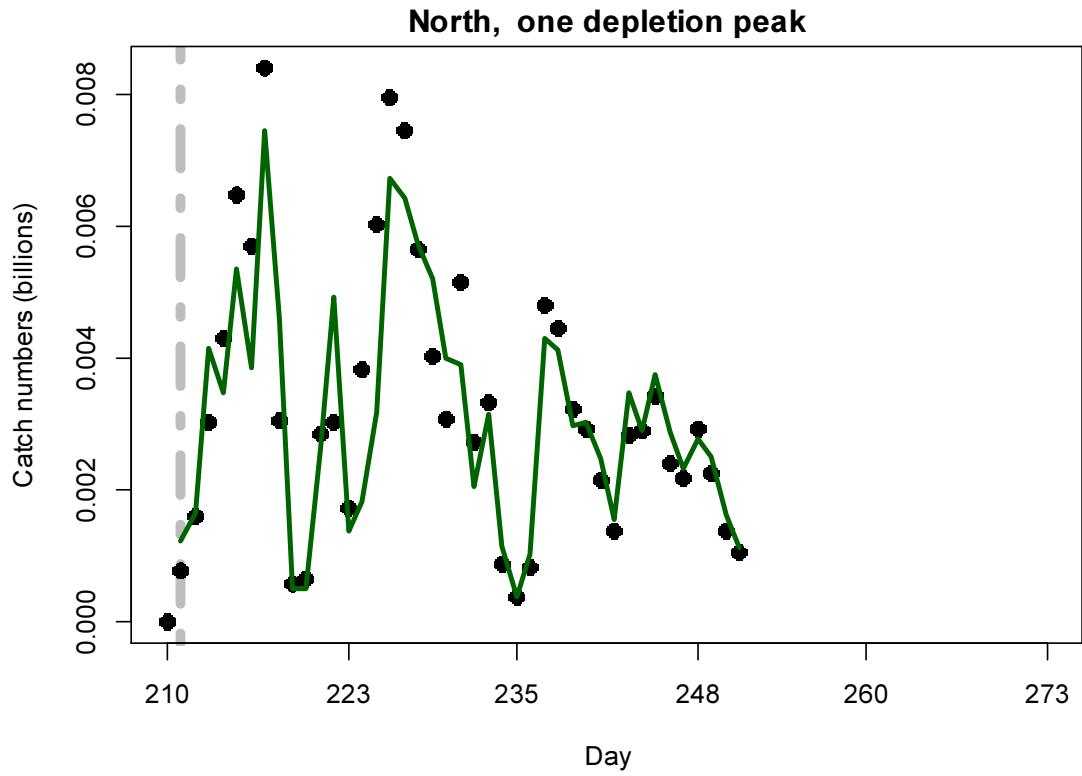


Figure A2-N. Daily catch numbers estimated from actual catch (black points) and predicted from the depletion model (green line) in the north sub-area.

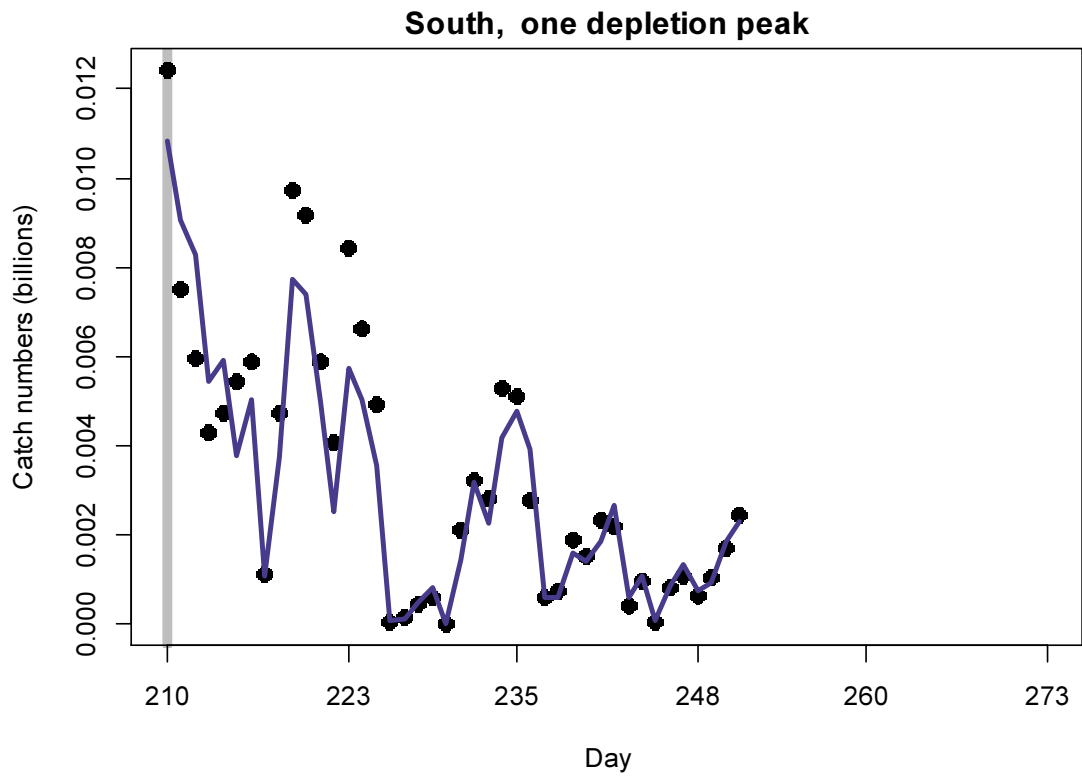


Figure A2-S. Daily catch numbers estimated from actual catch (black points) and predicted from the depletion model (blue line) in the south sub-area.